ISSN 1009 – 3095 *Journal of Zhejiang University SCIENCE* V.4, No.3, P.317 – 323, May – June, 2003
http://www.zju.edu.cn/jzus; http://www.periodicals.com.cn; jzus@zju.edu.cn

Geometrical nonlinear stability analyses of cable-truss domes*

GAO Bo-qing(高博青)†, LU Qun-xin(卢群鑫), DONG Shi-lin(董石麟)
(*Department of Civil Engineering, Zhejiang University, Hangzhou 310027, China*)
†E-mail: bqgao@zjuem.zju.edu.cn
Received July 15, 2002; revision accepted Oct. 20, 2002

Abstract: The nonlinear finite element method is used to analyze the geometrical nonlinear stability of cable-truss domes with different cable distributions. The results indicate that the critical load increases evidently when cables, especially diagonal cables, are distributed in the structure. The critical loads of the structure at different rise-span ratios are also discussed in this paper. It was shown that the effect of the tensional cable is more evident at small rise-span ratio. The buckling of the structure is characterized by a global collapse at small rise-span ratio; that the torsional buckling of the radial truss occurs at big rise-span ratio; and that at proper rise-span ratio, the global collapse and the lateral buckling of the truss occur nearly simultaneously.

Key words: Cable-truss dome, Geometrical nonlinear stability analysis, Parameter analysis, Cable distribution, Critical load
Document code: A **CLC number:** TU393.99

INTRODUCTION

The tensegrity structure composed of cables and bars is of two types. One is the flexible tensegrity structure. This type of structure has no stiffness and the shape of the structure is not determined when no prestress is applied. The form-finding process for the initial equilibrium is a significant problem for this type of structure (Liu *et al.*, 1995; Hangai *et al.*, 1981). Another is the "rigid" tensegrity structure, for example the cable-truss dome. Even if no prestress is applied, the shape of this type of structure can be determined. But the structure performance can be improved when the cables are distributed properly. The cable-truss dome commonly consists of trusses and cables. Up to now, its planar arrangement has been mostly restricted to rectangular form. In practical engineering, the Anhui gymnasium and the Chaozhou gymnasium are the only large cable-truss domes in our country (Xie *et al.*, 1989). Studies on cable-truss domes mostly focus on the static and dynamic properties and the structural design parameters and earthquake responses, while no nonlinear stability researches are carried out (Wang *et al.*, 1999; Cao *et al.*, 1991). Thus, either the theory or the practical engineering needs further studies. In this paper, a new circular cable-truss structure looking like a rib-ring reticulated dome is put forward. In this type of structure, the radial trusses are planarly or spatially distributed and may be cut down at the joints of the radial and latitudinal trusses when the trusses are too dense. Except for the outer latitudinal truss, the latitudinal truss is usually planar. The tensional cables are distributed latitudinally through the nodes of the top chords and bottom chords of the radial trusses, while the diagonal cables are distributed between the radial trusses to improve the stability of the structure. Planar trusses may be substituted for space trusses in larger structures. As Figs.1a and 1b shows, the structure is concise and lucid compared with normal reticulated domes. In this work, the effects of cable distributions on the geometrical nonlinear stability of the structure were studied by comparison with the relevant truss dome. The results indicated that properly distributing the latitudinal cables and diagonal cables can effectively prevent the lateral buckling of trusses and improve the stability of the structure. Geometrical nonlinear stability

* Project (No.50278086) supported by the National Natural Science Foundation of China

analyses of the structure at different rise-span ratios showed that perfect bearing capacity could be achieved at a proper rise-span ratio.

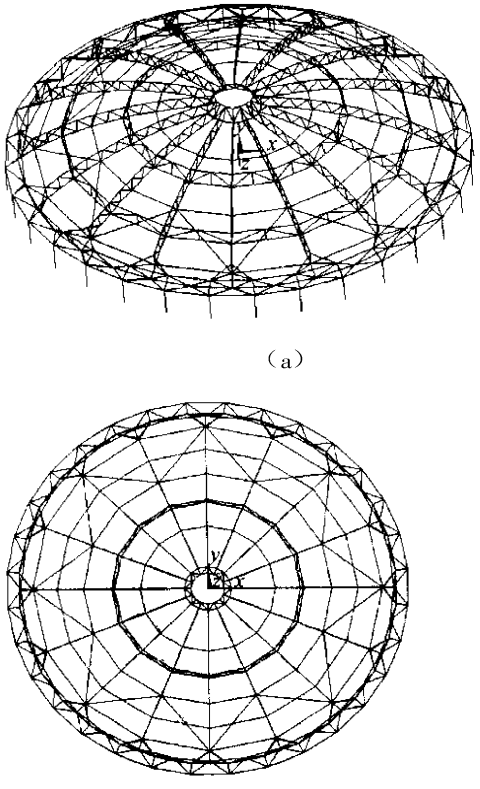

(a)

(b)

Fig.1 The cable-truss dome
(a) scenograph; (b) planform

Structural analysis method

The cable-truss dome consists of cables, beams and bars. The cable can be analyzed using the following methods: 1. Equivalent elastic modulus method (Kaid *et al*., 1999; Karoumi *et al*., 1996; Walther *et al*., 1988). It is a linear analysis method adopting bar elements to simulate cable segments. The deflection of cables is included in the equivalent elastic modulus and no stress stiffness and large displacement are included in this method. 2. Bar element method (Abdel-Ghaffar *et al*., 1991). Tension-only bar elements are used to simulate the curved cable in this method so that the number of cable segmentations is crucial to the precise solutions. 3. Catenary and parabola element methods (Aufaure, 2000). Catenary elements or parabola elements which include inertial deflection are used to simulate the curved cable. These elements have few freedoms and highly precise solutions for simulating cables, especially long cables with small tensional force. 4. Isoparametric element method (Leonard, 1988). Numerical integrations are needed in this method. The isoparametric element has few freedoms and highly precise solutions. 5. Consecutive slipping cable model (Zhang *et al*., 2000; 2001). The segments slipping of consecutive cables are included in this method. In this paper, the joints of cables and bars are assumed to be fixed, so the second cable mechanical model is adopted. The member can be analyzed by using the Oran method based on beam-column theory (includes the stability function) or by using the nonlinear finite element method or by using the isorotation method. The nonlinear finite element method includes the T.L (Total Lagrange) and U.L (Updated Lagrange) method. The U.L method is used in this paper. The stiffness matrixes of beam elements and bar elements in this method are detailed in Song (1996). The structure increment equilibrium equation may be expressed as

$$[K]\{\Delta \boldsymbol{u}\} = \Delta\lambda \{\boldsymbol{p}\} \tag{1}$$

Where $[K]$ is the structural tangent stiffness matrix of U.L, $\{\Delta \boldsymbol{u}\}$ is the increment vector of displacement, $\Delta\lambda$ is the load increment parameter, $\{\boldsymbol{p}\}$ is the load reference vector. Before the critical load, $|K| \neq 0$, thus, an exclusive solution of the linear Eq. (1) can be obtained by using LDLT. At the critical point, $|K| \neq 0$, rank $(K) \leqq n-1$, and the structural stiffness matrix is singular. On the basis of the generalized incremental algorithm (Hangai *et al*., 1981; Chen and Dong, 2001; Chen *et al*. 2002), the Eq. (1) can be written as:

$$A\begin{Bmatrix}\Delta\delta\\ \Delta\lambda\end{Bmatrix} = \{0\} \tag{2}$$

Where $A = [K - f]$, is the augmented equilibrium matrix with $n \times (n+1)$ dimensions.

By using the generalized inverse theory, the solution of the Eq. (2) is:

$$\begin{Bmatrix}\Delta\delta\\ \Delta\lambda\end{Bmatrix} = [I_{n+1} - A^{+}A]\boldsymbol{a} = \alpha\,\mathrm{null}(A) = \alpha\boldsymbol{a} \tag{3}$$

Where A^{+} is the *M-P* generalized inverse of A, $\boldsymbol{a}$ is the zero spatial radix and the orthogonal radix of $[I_{n+1} - A^{+}A]$. α is a number without dimensions, named the generalized increment. Regarding the physical significance, the conser-

vative structure has an exclusive equilibrium route at non-critical points and limit points so that $\boldsymbol{a}$ is a vector of one-dimension; while the conservative structure has two equilibrium routes at least at the bifurcation point so that $\boldsymbol{a}$ is a multi-dimensions vector. The results of nonlinear analyses showed that the cable-truss dome presented in this paper has no bifurcation points.

The tracking of load-displacement curves is a critical technology for analyzing nonlinear structures. The arc-length method is used to get the curves in this paper.

Geometrical nonlinear characteristics of cable-truss domes

Now we take the structure in Fig. 1 for example to analyze its geometrical nonlinear characteristics. The structure with 60 m span and 12 m rise consists of sixteen radial planar trusses and three latitudinal planar trusses and one outer latitudinal space truss and cables. In planar trusses, 165 × 6 mm tubes are used for the top chord and bottom chord and 89 × 4 mm tubes are used for web members. The members of the outer latitudinal space truss are 159 × 6 mm tubes. The prestress of the top latitudinal cable is 300 kN, the prestress of the bottom latitudinal cables from outer to inner cables is 600 kN, 200 kN, 300 kN respectively and the prestress of the diagonal cable is 100 kN. The structure bears uniformly-distributed load 2 kN/m^2. ANSYS is used to analyze this structure. 3-D beam element is used to simulate the top chord and the bottom chord of planar trusses. Bar element is used to simulate the web member and members of the outer latitudinal space truss. Tension-only bar element is used to simulate the cable. The arc-length method is used to get displacement-load curves.

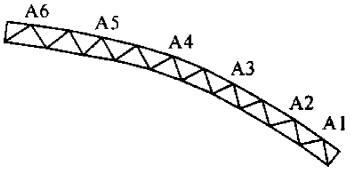

Fig. 2 Nodes location of the top chord

Fig. 3a shows vertical displacement-load curves of some nodes at the top chord of the buckling radial truss (nodes location are shown in Fig. 2), Fig. 3b shows the buckling mode of the structure without cables. The maximum vertical displacement is about 20 cm (only 1/750 span of the structure) before the first critical point after which the displacement of the structure increases rapidly. The buckling begins in the middle of radial trusses, subsequently extends to inner latitudinal trusses, and spreads over around until the lateral buckling that occurs in the radial and latitudinal trusses leads collapse of the structure. The critical load is low, just 5.311 kN/m^2.

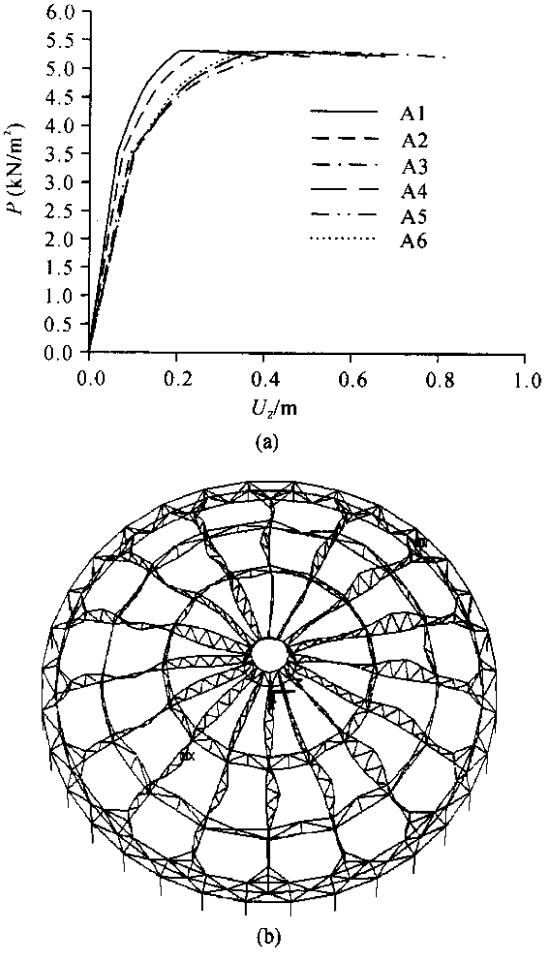

Fig. 3 mode of The structure without cables
(a) vertical displacement-load curve; (b) buckling mode

Fig. 4a shows vertical displacement-load curves of some nodes at the top chord of the buckling radial truss. Fig. 4b shows the buckling mode of the structure with three bottom latitudinal cables. The buckling process is similar to that of the structure without cables. The critical load is 6 kN/m^2. Though the increment is 13%

compared with that of the structure without cables, the bulking is still unsymmetrical local collapse. Thus, the improving of structure performances is little when only bottom latitudinal cables are distributed in the structure because the minimal lateral restrictions on top chords of the truss leads to the earlier lateral buckling.

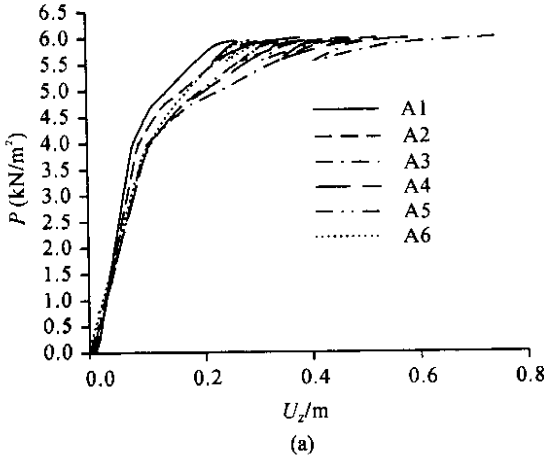

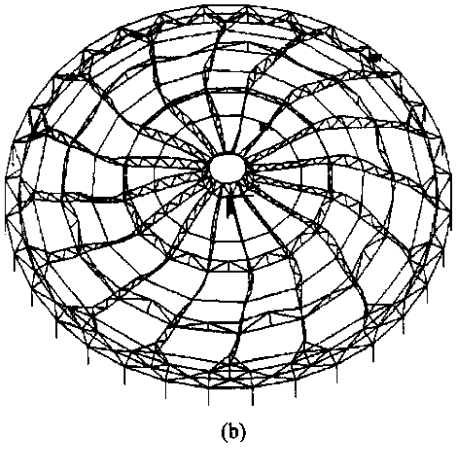

Fig.4 The structure with three bottom latitudinal cables
(a) vertical displacement-load curve; (b) buckling mode

Fig.5a shows vertical displacement-load curves of some nodes at the top chord of the buckling radial truss, Fig.5b shows the buckling mode of the structure with diagonal cables. The results of numerical analyses showed that the slack of some cables leads to a decrease of the stiffness so that a brief unloading occurs (one substep) when the load of the structure reaches 4.23 kN/m^2, subsequently, these slack cables are tensed again and the stiffness of the structure is redistributed and the loading continues. The buckling process is also similar to that of the structure without cables. But the buckling is symmetrical and the displacement wave is smooth. The critical load is 6 kN/m^2. Thus, we can conclude that the diagonal cables improve the performances of the structure.

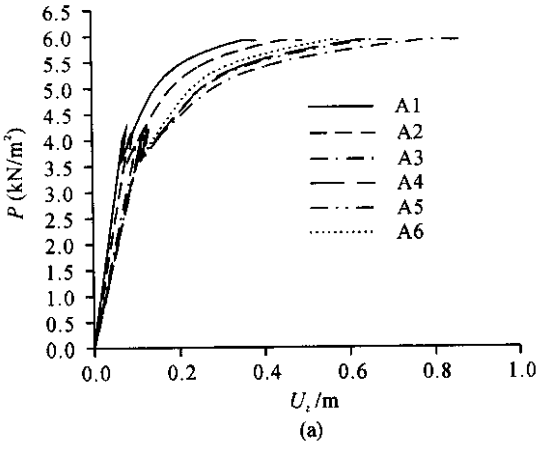

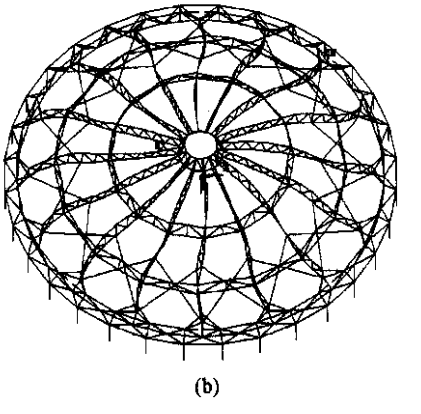

Fig.5 The structure with diagonal cables
(a) vertical displacement-load curve; (b) buckling mode

Fig.6a shows vertical displacement-load curves of some nodes at the top chord of the buckling radial truss, Fig.6b shows the buckling mode of the structure with two top latitudinal cables and three bottom latitudinal cables. The buckling begins in the middle of the radial truss, subsequently spreads over around smoothly. The bulking is still a local collapse, the displacement wave is very smooth and the critical load is 7.5 kN/m^2 (the increment is 41% compared with that of the structure without cables). Thus, the structure performances are improved greatly when

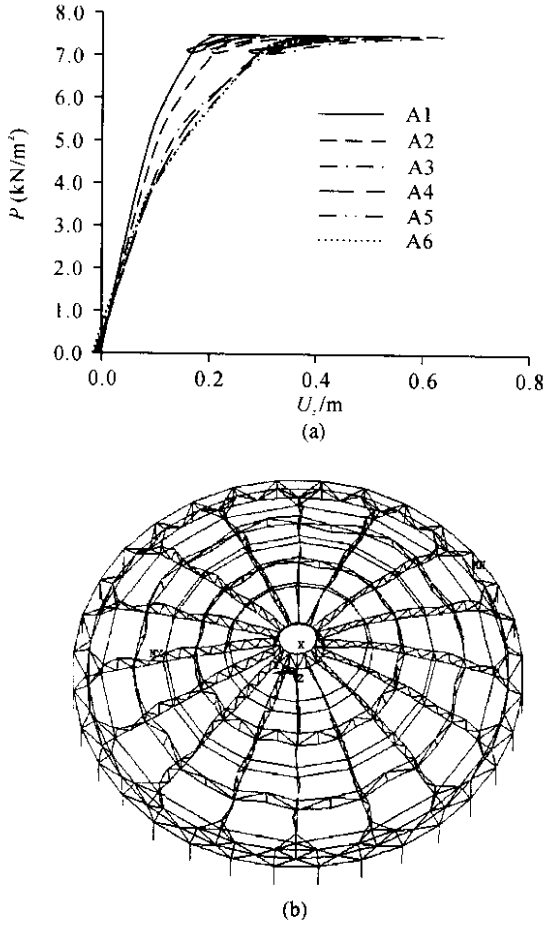

Fig.6 The structure with two top latitudinal cables and three bottom latitudinal cables
(a) vertical displacement-load curve; (b) buckling mode

both top and bottom latitudinal cables are distributed in the structure because the cable restrictions on the top chords and bottom chords of the truss can prevent the earlier lateral buckling of the truss. Therefore, the critical load of this structure is much higher than that of the structure with three bottom latitudinal cables. The results of numerical analyses showed that a slackening of some cables occurs after the buckling of the structure so that the stiffness of the structure is minimal and the displacement increases rapidly. Subsequently, the slack cables are tensed again when the displacement is big enough and the stiffness increases slowly so that the displacement decreases and "spring-back" occurs (As shown in Fig.4 and Fig.6).

Fig.7a shows vertical displacement-load curves of some nodes at the top chord of the buckling radial truss, Fig.7b shows the buckling mode of the structure with five latitudinal cables (two top latitudinal cables and three bottom latitudinal cables) and diagonal cables. Compared with Fig.6, the beginning of the buckling takes place in the inner latitudinal truss and the buckling is a global collapse. Meanwhile, the critical load is 8.28 kN/m^2 and the increment is 56% compared with that of the structure without cables. The results showed that the diagonal cable can prevent the lateral buckling of truss and improve the stability performance of the structure.

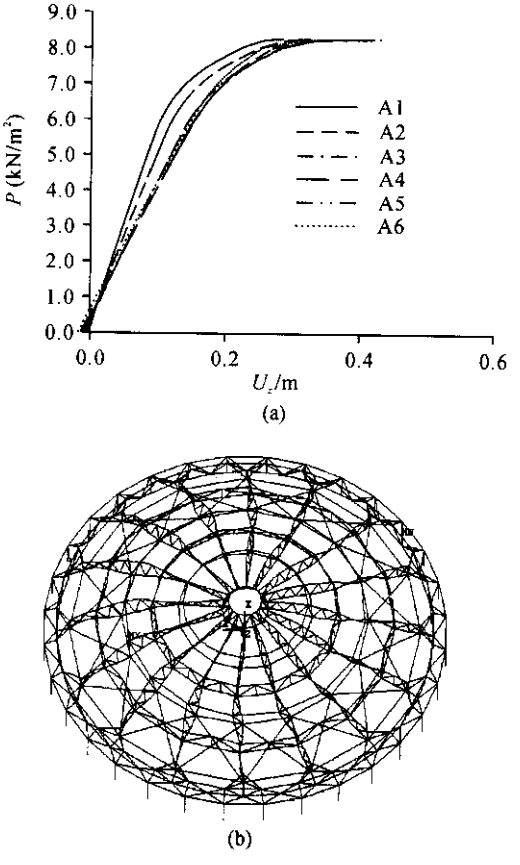

Fig.7 The structure with five latitudinal cables(two top latitudinal cables and three bottom latitudinal cables) and diagonal cables
(a) vertical displacement-load curve; (b) buckling mode

Some conclusions can be drawn from above discussions: distributing top and bottom latitudinal cables and diagonal cables can prevent the earlier lateral buckling of truss and improve the stability performance of the structure (the diagonal cable is the most important); the strengthening of the structure is not evident after the buckling and some signs can be seen before the buckling; the beginning of the buckling usually takes place in the middle of radial truss or in the inner

latitudinal truss.

The effect of the rise-span ratio on the stability performance of cable-truss domes

Now we take the structure in Fig.7 as example to discuss the effect of the rise-span ratio on the stability performance of the cable-truss dome. Keeping the span constant, we consider five rises (f): 8 m, 10 m, 12 m, 14 m, 16 m. The displacement-load curves and buckling modes at the five rise-span ratios are shown in Fig.8. – Fig.13. From Fig.8, we can know that the structure has optimal rise-span ratio. The critical load is the maximum when the rise-span ratio is 1/6. Different from the normal reticulated dome, this structure does not be strengthened after the buckling. In Fig. 9 , it is shown that global collapse occurs earlier than the lateral buckling because of the proper distribution of latitudinal and diagonal cables; and that the vertical displacement is much greater than the horizontal when the buckling occurs. In Fig. 10, it is shown that the difference between the vertical displacement and the horizontal displacement is small so that global collapse and lateral buckling of the truss occur nearly simultaneously at 10 m rise. Thus, the critical load is the maximum of the ones at five rise-span ratios. In Fig.11, it is shown that the horizontal displacement is greater than the vertical displacement of the structure at 12 m rise at first; and that the difference is small when the load reaches 8 kn/m^2. Thus, the buckling begins in the latitudinal truss; then global buckling occurs. The critical load is less than that of the previous structure. In Fig. 12 and Fig.13, it is shown that lateral buckling and torsional buckling of the radial truss occur; and that the critical load decreases evidently at rise 14 m and 16 m, which differ from the normal reticulated dome.

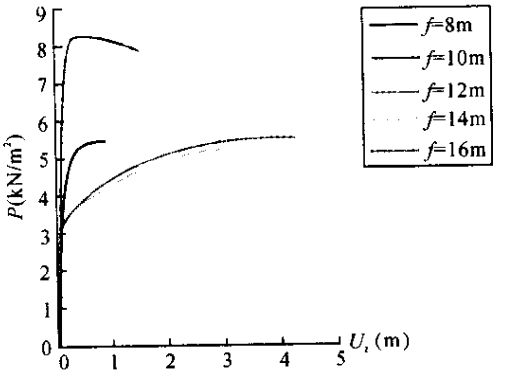

Fig.8 The displacement-load curves at five rise-span ratios

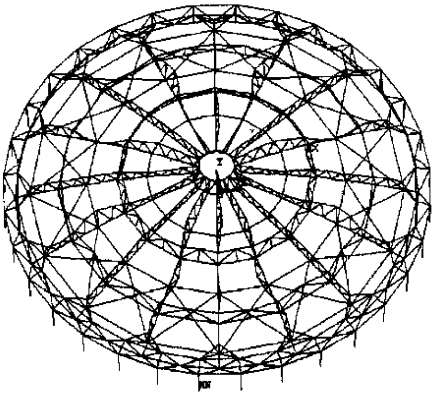

Fig.9 The buckling mode at 8 m rise

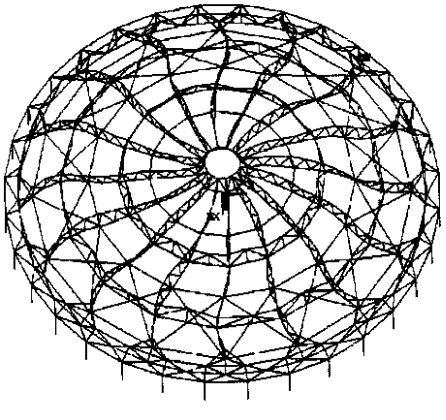

Fig.10 The buckling mode at 10 m rise

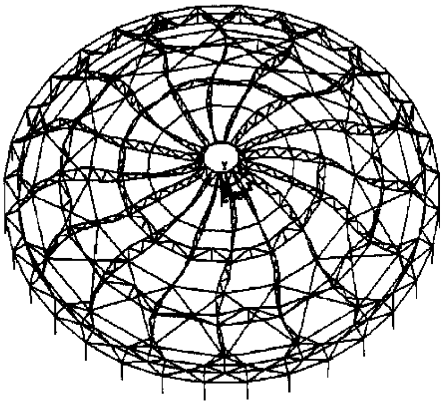

Fig.11 The buckling mode at 12 m rise

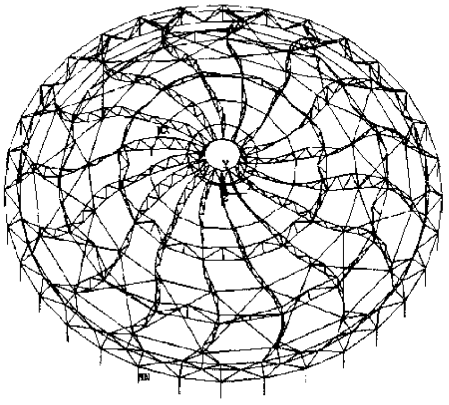

Fig.12 The buckling mode at 14 m rise

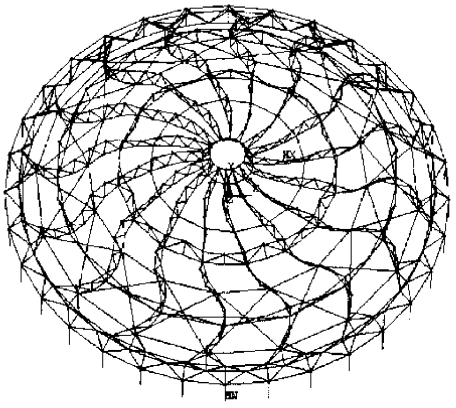

Fig.13 The buckling mode at 16 m rise

CONCLUSIONS

1. The cable-truss dome put forward in this paper has good performance.

2. Proper distribution of top and bottom latitudinal cables and diagonal cables can prevent the earlier lateral buckling of truss and improve the stability performance of the structure (the diagonal cable is the most important).

3. The strengthening of the structure is not evident after the buckling and some signs can be seen before the buckling. The buckling usually begins in the middle of the radial truss or in the inner latitudinal truss.

4. The buckling mode relates closely to the rise-span ratio of the structure. The buckling of the structure is a global collapse at small rise-span ratio and the torsional buckling of the radial truss occurs at big rise-span ratio and at proper rise-span ratio (1/6 for the case in this paper), the global collapse and the lateral buckling of the truss occur nearly simultaneously so that the structure can bear the maximum load.

References

Abdel-Ghaffar, A.M. and Khalifa, M.A., 1991. Importance of cable vibration in dynamics of cable-stayed bridges. *Journal of Engineering Mechanics, ASCE*, **117**: 2571-2589.

Aufaure, M., 2000. A three-node cable element ensuring the continuity of the horizontal tension: a clamp cable element. *Computers & Structure*, **74**: 243 – 251.

Cao, Z. and Ketter, R.L., 1991. Seismic modeling of Truss Stiffened Cable System. *International Journal of Space Structure*, **6**(1): 18 – 25.

Chen, W.J. and Dong, S.L., 2001. Generalized incremental algorithm for nonlinear structural analysis. *Engineering Mechanics*, **18**(3): 28 – 33(in Chinese).

Chen, W.J., Fu, G.Y., Gong, J.H. and Dong, S.L., 2002. Instability behavior of partial double-layer lattice-ribbed domes. *Spatial structure*, **8**(1): 19 – 28(in Chinese).

Hangai, Y., 1981. Application of the generalized inverse to the geometrically nonlinear problem. *Solid Mechanics (SM) Archives*, **6**(1): 129 – 165.

Hangai, Y. and Kawaguchi, K., 1990. Analysis for shape-finding process of unstable structures. *Bulletin of IASS*, **30**(100): 111 – 128

Karoumi, R., 1996. Dynamic response of cable-stayed bridges to moving vehicles. IABSE 15th Congress, Denmark, p.87 – 92.

Karoumi, K., 1999. Some modeling aspects in the nolinear finite element analysis of cable supported bridges. *Computers & Structures*, **71**(1): 397 – 412.

Leonard, J.W., 1988. Tension Structure. McGraw-Hill, New York.

Liu, Y. and Motro, R., 1995. Shape analysis and internal forces in unstable structures. Proc. IASS Int. Symposium, **2**: 819 – 826.

Song, T.X., 1996. Finite element analysis of nonlinear structures. Press of Huazhong University of science and technology, Wuhan(in Chinese).

Walther, R., Houriet, B., Isler, W. and Moia P., 1988. Cable Stayed Bridges. Thomas Telford, London.

Wang, S.T. and Jiang, Z.R., 1999. The static analysis and study of dynamic characteristics of the cable-truss structure. *Journal of Building structure*, **20**(3): 2 – 7 (in Chinese).

Xie, Y.Z. and Chen, Q.Z., 1989. Design and construction of the cable-truss. *Composite structure of Anhui gymnasium*, **10**(6): 71 – 79(in Chinese).

Zhang, L.X. and Shen, Z.Y., 2000. Numerical models for cable element in prestressed cable structures. *Spatial structure*, **6**(2): 18 – 23(in Chinese).

Zhang, Z.H. and Dong, S.L., 2001. Slippage analysis of continuous cable in tension structures. *Spatial structure*, **7**(3): 26 – 32(in Chinese).